Unidirectional flow of a thin rivulet on a vertical substrate subject to a prescribed uniform shear stress at its free surface

S. K. Wilson and **B. R. Duffy**
Department of Mathematics, University of Strathclyde, Livingstone Tower, 26 Richmond Street, Glasgow G1 1XH, United Kingdom

We use the lubrication approximation to obtain a complete description of the steady unidirectional flow of a thin rivulet on a vertical substrate subject to a prescribed uniform longitudinal shear stress at its free surface. We interpret the solution we obtain both as a rivulet with prescribed semi-width but unknown flux, and as a rivulet with prescribed flux but unknown semi-width. We systematically categorise and analyse all of the possible flow patterns and find that whereas when the prescribed shear stress acts downwards the velocity is always downwards throughout the rivulet, when the prescribed shear stress acts upwards the velocity is always upwards near the edges of the rivulet, but it can be downwards elsewhere. In particular, when the rivulet is sufficiently narrow the velocity is always upwards throughout the rivulet. We also determine the quasi-steady stability of a rivulet in the case of prescribed flux, and calculate when it is energetically favourable for a rivulet to split into two narrower rivulets.

1 Introduction

Layers of fluid subject to significant forces at their free surface due to an external airflow occur in a wide variety of practical situations, and as a result there has been considerable theoretical work on a variety of such flows. Examples include the work by Moriarty, Schwartz and Tuck [1] on the unsteady spreading of a thin fluid film with weak surface tension subject to an external airflow, the work by King and Tuck [2] and King, Tuck and Vanden-Broeck [3] on a thin film of fluid supported against gravity on an inclined plane by an upward airflow, the work by Kriegsmann, Miksis and Vanden-Broeck [4] on the effect of a steadily moving pressure disturbance on a thin fluid film on an inclined plane, the work by McKinley, Wilson and Duffy [5] on a thin ridge or droplet of fluid subject to a jet of air, the work by Myers, Charpin and Thompson [6] on the growth of ice due to droplets of supercooled fluid impacting on a cold substrate, and the work by Villegas-Díaz, Power and Riley [7], Black [8], and Wilson, Duffy and Black [9] on a thin film of fluid on a horizontal cylinder subject to a uniform shear stress due to an external airflow.

In particular, rivulets of fluid subject to significant surface-shear forces occur in a variety of contexts, including the rivulets of rainwater and/or deicing fluid that form on the wings of aircraft (see, for example, Myers *et al.* [6]), the rivulets of condensate that frequently occur within heat exchangers (see, for example, Saber and El-Genk [10]), and even the rivulets of rainwater that can be observed on the windscreen of a rapidly moving car on a rainy day! These applications have motivated a number of authors to use a variety of theoretical and numerical approaches to address various aspects of this practically important problem. Mikielewicz and Moszynski [11] analysed the breakup of a fluid film into rivulets by comparing the energy of the film with the energy of the possible rivulet configurations. In particular, they considered the unidirectional flow of a rivulet on an inclined plane driven either by gravity or by a uniform shear stress at its free surface. Eres, Schwartz and Roy [12] analysed the unsteady fingering phenomena that occur at the contact line of a thin fluid film on an inclined plane driven either by gravity or by a uniform shear stress at its free surface. They formulated the unsteady partial differential equation governing the evolution of the film and solved it numerically. Their calculations showed that for partially wetting systems with sufficiently large static contact angles the final state is of long, straight-sided rivulets of the kind analysed in the present work. Wilson, Duffy and Hunt [13] obtained similarity solutions for slender

non-uniform rivulets of Newtonian and a non-Newtonian power-law fluid on an inclined plane driven either by gravity or by a uniform shear stress at its free surface. In particular, when surface tension is weak they found that there is a unique similarity solution representing both a widening and shallowing sessile rivulet and a narrowing and deepening pendent rivulet; on the other hand, when surface tension is strong they found that there are one-parameter families of solutions representing a widening and shallowing rivulet, and a narrowing and deepening rivulet, respectively. Recently Myers, Liang and Wetton [14] investigated the unidirectional flow of a rivulet on an inclined plane subject to a prescribed uniform longitudinal shear stress at its free surface. They solved the problem asymptotically for thin rivulets and numerically, and found that the asymptotic solution is in good agreement with the numerical solution for values of the contact angle up to about 30°. In addition, following an approach suggested by Schmuki and Laso [15], Myers *et al.* [14] calculated when it is energetically favourable for a purely gravity-driven rivulet to split into two narrower rivulets. They also conjectured that it is never energetically favourable for a purely shear-stress-driven rivulet to split in this manner. In the present work we shall show that this conjecture is not correct, and calculate when it is energetically favourable for a rivulet on a vertical substrate driven by gravity and/or a prescribed shear stress to split. Saber and El-Genk [10] analysed the unidirectional flow of a rivulet on an inclined plane subject to a longitudinal shear stress at its free surface. In contrast to the works described above, the shear stress was not assumed to be uniform, but was instead taken to be a function of the uniform velocity of the airflow above the rivulet and the non-uniform interfacial velocity of the rivulet. Saber and El-Genk [10] investigated the effect of the external airflow on the breakup of a fluid film into rivulets, and found good agreement between their predictions and the experimental results of previous authors.

In the present paper we use the lubrication approximation to obtain a complete description of the steady unidirectional flow of a thin rivulet on a vertical substrate subject to a prescribed uniform longitudinal shear stress at its free surface.

2 Problem Formulation and Solution

Consider the steady unidirectional flow of a thin symmetric rivulet with constant semi-width a and constant volume flux Q on a vertical substrate subject to a prescribed uniform longitudinal shear stress τ at its free surface. Note that positive (negative) values of τ correspond to the prescribed shear stress acting downwards (upwards), and that the flux Q may be either positive or negative, indicating a net downwards or upwards flow, respectively. We assume that the fluid is Newtonian and has constant density ρ, viscosity μ and surface tension γ. We choose Cartesian axes $Oxyz$ with the x axis vertically downwards, the y axis horizontal and parallel to the substrate $z = 0$, and the z axis horizontal and normal to the substrate. The velocity $\mathbf{u} = u(y, z)\mathbf{i}$ and pressure $p = p(x, y, z)$ of the fluid are governed by the familiar mass-conservation and Navier–Stokes equations subject to the usual normal and tangential stress balances and the kinematic condition at the (unknown) free surface $z = h(y)$, and zero velocity at the substrate $z = 0$. At the contact line $y = a$ where $h = 0$ the contact angle takes the prescribed value β, where $\beta > 0$ is the (non-zero) static contact angle.

Analytical progress can be made when the rivulet is thin (with, in particular $\beta \ll 1$) in which case it is appropriate to non-dimensionalise y and a with l, z and h with βl, u with $U = \rho g \beta^2 l^2/\mu$, Q with $\beta l^2 U = \rho g \beta^3 l^4/\mu$, $p - p_\infty$ with $\rho g \beta l$, and τ with $\rho g \beta l$, where $l = (\gamma/\rho g)^{1/2}$ is the capillary length, g is gravitational acceleration and p_∞ is the uniform pressure in the surrounding atmosphere. Henceforth all quantities are non-dimensional unless stated otherwise. The leading-order versions of the Navier–Stokes equations are simply

$$0 = 1 + u_{zz}, \quad 0 = -p_y, \quad 0 = -p_z, \tag{1}$$

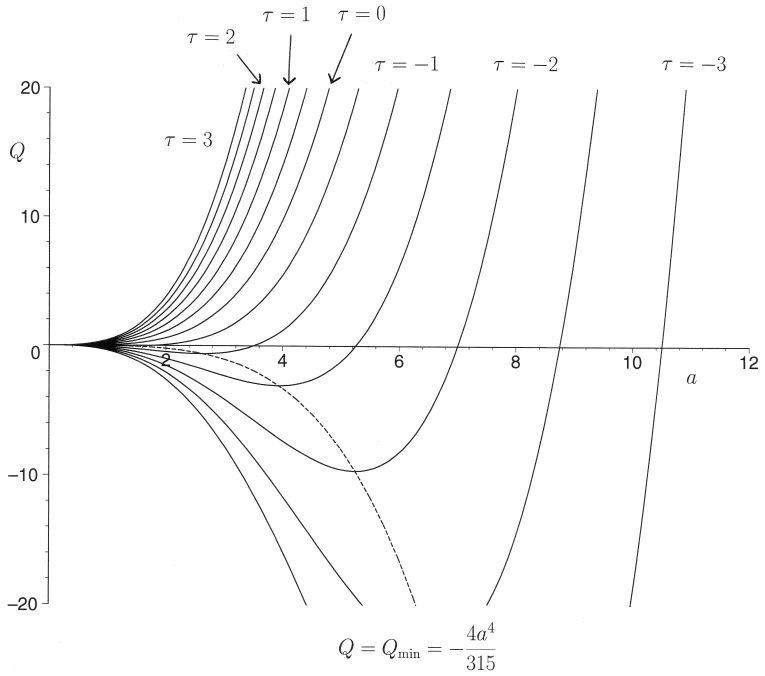

Figure 1: Plot of Q as a function of a for $\tau = -3, -5/2, -2, \ldots, 3$. The locus of the minima, $Q = Q_{\min} = -4a^4/315$, is indicated with a dashed line.

and the leading-order versions of the boundary conditions are

$$u = 0 \quad \text{on} \quad z = 0, \tag{2}$$

$$p = -h'' \quad \text{and} \quad u_z = \tau \quad \text{on} \quad z = h, \tag{3}$$

$$h = 0 \quad \text{and} \quad h' = \mp 1 \quad \text{at} \quad y = \pm a. \tag{4}$$

Note that since the flow is unidirectional, the mass-conservation equation and the kinematic condition are satisfied identically, and (since the inertia terms are all identically zero) the solution given below is valid for *all* values of the Reynolds number. Solving the equations (1) subject to the boundary conditions (2)–(4) immediately yields the simple solution

$$p = -h'' = \frac{1}{a}, \quad u = \frac{(2h - z)z}{2} + \tau z, \quad h = \frac{a^2 - y^2}{2a}, \tag{5}$$

showing that the pressure is uniform across the rivulet and determined by the force due to surface tension at the free surface, that the velocity is a combination of a parabolic profile due to gravity and a linear profile due to the prescribed shear stress at the free surface, and that the profile of the rivulet is a simple parabolic shape due to surface tension. In particular, the maximum thickness of the rivulet occurs at $y = 0$ and is equal to $h_{\mathrm{m}} = h(0) = a/2$. The free-surface velocity $u_{\mathrm{S}} = u_{\mathrm{S}}(y)$, local flux $\bar{u} = \bar{u}(y)$ and the flux Q are given by

$$u_{\mathrm{S}} = u(y, h) = \frac{h^2}{2} + \tau h, \tag{6}$$

$$\bar{u} = \int_0^h u(y, z)\,\mathrm{d}z = \frac{h^3}{3} + \frac{\tau h^2}{2} \tag{7}$$

and

$$Q = \int_{-a}^{+a} \bar{u}(y)\,\mathrm{d}y = \frac{4a^4}{105} + \frac{2\tau a^3}{15}, \tag{8}$$

respectively. Note that the expression for Q is in agreement with the appropriate limit of the corresponding result given by Myers *et al.* [14, Equation 25]. Figure 1 shows Q plotted as a function of a for a range of values of τ and illustrates that for $\tau \geq 0$ it is a monotonically increasing function of a, but for $\tau < 0$ it initially decreases monotonically to a minimum value of $Q = Q_{\min}$ (< 0), where

$$Q_{\min} = -\frac{4a_{\min}^4}{315} = -\frac{3087\tau^4}{5120}, \tag{9}$$

at $a = a_{\min} = -21\tau/8$, before increasing monotonically through the value $Q = 0$ at $a = a_0 = -7\tau/2$. Whatever the sign of τ, $Q = O(a^3)$ (or $O(a^4)$ in the special case $\tau = 0$) as $a \to 0^+$ and $Q = O(a^4) \to \infty$ as $a \to \infty$.

The solution described above can be interpreted in two different ways. The simplest interpretation (adopted by, for example, Myers *et al.* [14] and Saber and El-Genk [10]) is to assume that the semi-width of the rivulet takes a prescribed value $a = \bar{a}$, in which case the corresponding flux is then given explicitly by (8). Figure 2 shows Q plotted as a function of τ for a range of values of $\bar{a}$. Note that each curve is a straight line and the envelope curve is $Q = Q_{\min} = -3087\tau^4/5120$ in $\tau \leq 0$. Another equally sensible interpretation (adopted by, for example, Duffy and Moffatt [16] and Wilson and Duffy [17] in their analyses of a gravity-driven rivulet draining down a slowly varying substrate) is to assume that the flux takes a prescribed value $\bar{Q}$, in which case the possible semi-widths are the positive solutions of $Q = \bar{Q}$, where Q is given by (8). Figure 3 shows a plotted as a function of τ for a range of values of $\bar{Q}$. In either case, once the value of a is known, the corresponding solutions for p, u and h are given explicitly by (5). In the remainder of the present work we will describe the behaviour of the possible rivulet solutions in both of these scenarios.

3 Flow Patterns

In their study of unidirectional rivulet flow on an inclined plane Myers *et al.* [14] correctly identified that for relatively weak upwards shear there is a region of downwards flow near the centre of the rivulet, and that for sufficiently strong upwards shear this region disappears entirely resulting in upwards flow throughout the rivulet. Broadly similar results were obtained by Saber and El-Genk [10] for the problem they addressed. In this section we systematically categorise and analyse all of the possible flow patterns for the present problem. The five different types of flow pattern that can occur are referred to as type I to type V behaviour, and are sketched in Figure 4.

When $\tau > 0$ the prescribed shear stress acts downwards and hence augments the downward force of gravity. In this case the velocity is always downwards (i.e. $u > 0$) throughout the rivulet, and the maximum velocity $u_{\max} = u_{\rm s}(0) = a(a + 4\tau)/8$ (> 0) occurs on the free surface at $y = 0$ and $z = h_{\rm m} = a/2$. We refer to this simple flow pattern as type I behaviour (Figure 4a).

On the other hand, when $\tau < 0$ the prescribed shear stress acts upwards and hence opposes the downwards force of gravity. This competition between the effects of gravity and prescribed shear stress leads to more interesting behaviour than in the case $\tau > 0$. In particular, in the special case $a = a_0 = -7\tau/2$ there is a non-trivial solution with zero flux in which the downwards flux due to gravity is exactly equal to the upwards flux due to the prescribed shear stress; this is somewhat similar to the solution for a thin film of fluid supported against gravity on an inclined plane by an upward airflow analysed by King and Tuck [2] and King, Tuck and Vanden-Broeck [3].

In contrast to the case $\tau > 0$, in the case $\tau < 0$ the velocity is always upwards (i.e. $u < 0$) near the edges of the rivulet, but it can be downwards (i.e. $u > 0$) elsewhere. Specifically,

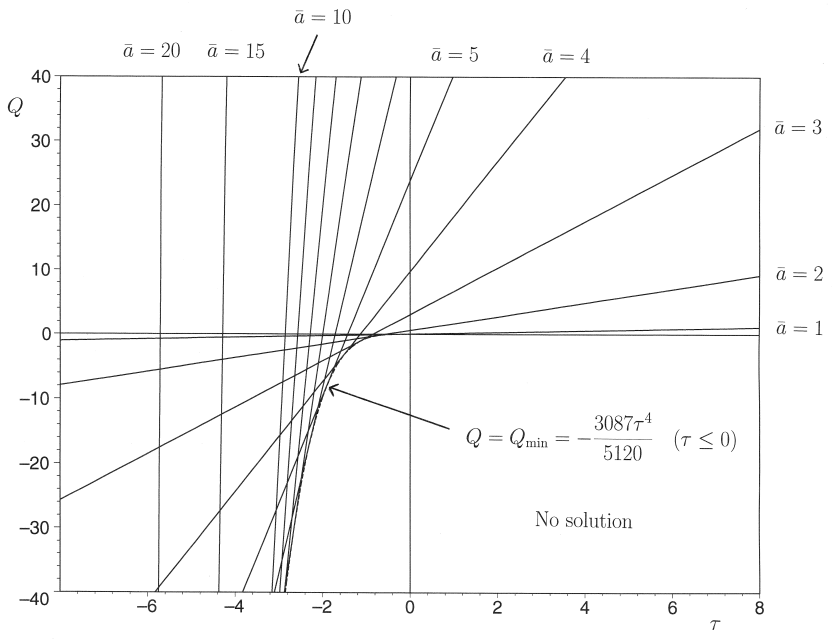

Figure 2: Plot of Q as a function of τ for $\bar{a} = 1$, 2, 3, 4, 5, 6, 7, 8, 9, 10, 15, 20. The envelope curve $Q = Q_{\min} = -3087\tau^4/5120$ in $\tau \le 0$ is indicated with a dashed line.

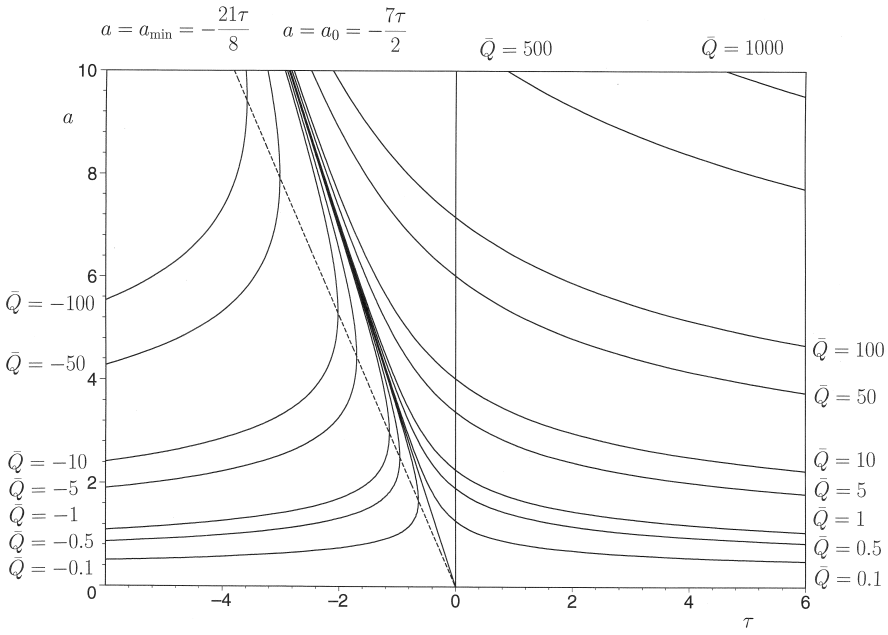

Figure 3: Plot of a as a function of τ for $\bar{Q} = -100$, -50, -10, -5, -1, -0.5, -0.1, 0, 0.1, 0.5, 1, 5, 10, 50, 100, 500, 1000. Note that $a = a_0 = -7\tau/2$ in the special case $\bar{Q} = 0$. The curve $a = a_{\min} = -21\tau/8$ is indicated with a dashed line.

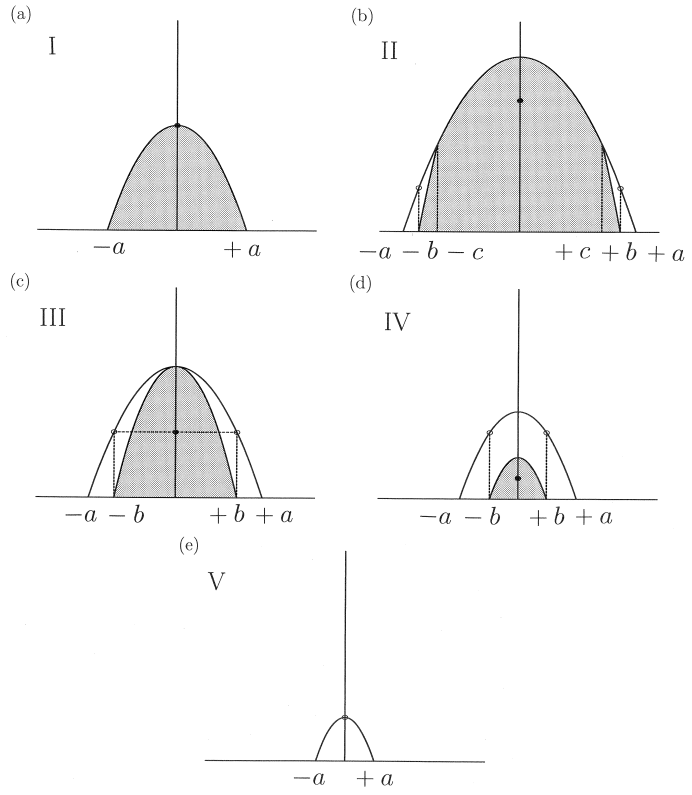

Figure 4: Sketches of the flow in the cases (a) $\tau > 0$ (type I), (b) $\tau < 0$ and $a > -4\tau$ (type II), (c) $\tau < 0$ and $a = -4\tau$ (type III), (d) $\tau < 0$ and $-2\tau < a < -4\tau$ (type IV), and (e) $\tau < 0$ and $a \leq -2\tau$ (type V). In each part regions of downwards flow (i.e. $u > 0$) are shaded in grey while regions of upwards flow (i.e. $u < 0$) are unshaded. The locations of the maximum and/or minimum velocity are marked with dots ($\bullet$) and/or open circles ($\circ$), respectively.

the curve on which the velocity is zero (which may or may not lie within the flow), denoted by $H = H(y)$, is given by

$$H = 2(h + \tau) = \frac{a(a + 2\tau) - y^2}{a}. \tag{10}$$

In particular, $H_{\rm m} = H(0) = a + 2\tau$. Note that $H = 0$ at $y = \pm b$, where

$$b = a\left(1 + \frac{2\tau}{a}\right)^{\frac{1}{2}} \tag{11}$$

(which lie within the flow when $a > -2\tau$), and $H = h$ at $y = \pm c$, where

$$c = a\left(1 + \frac{4\tau}{a}\right)^{\frac{1}{2}} \tag{12}$$

(which lie within the flow when $a > -4\tau$).

When $a > -4\tau$ we have $H_{\rm m} > h_{\rm m}$ and the velocity is downwards in the regions

$$0 < z < H \quad \text{for} \quad c < |y| < b \quad \text{and} \quad 0 < z \leq h \quad \text{for} \quad |y| < c, \tag{13}$$

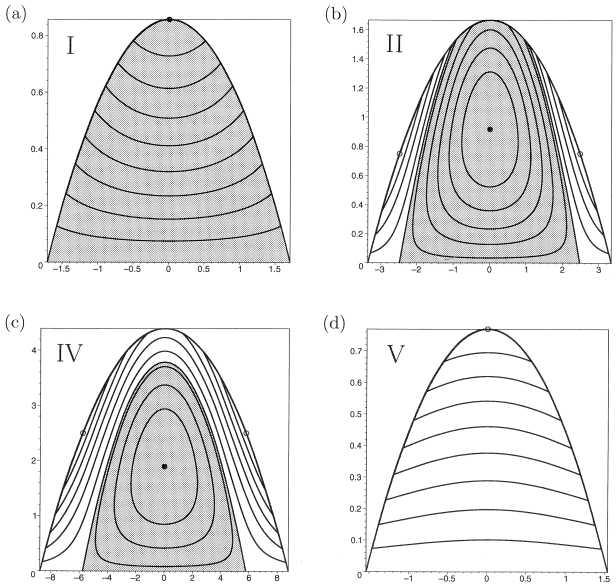

Figure 5: Plots of the contours of u in the cases (a) $Q = 1$, $\tau = 1$, $a \simeq 1.7139$ (type I), (b) $Q = 1$, $\tau = -3/4$ ($\tau_2 < \tau < 0$), $a \simeq 3.3336$ (type II), (c) $Q = -1$, $\tau = -5/2$ ($\tau < \tau_1$), $a \simeq 8.7103$ (type IV), and (d) $Q = -1$, $\tau = -5/2$ ($\tau < \tau_1$), $a \simeq 1.5383$ (type V). In each part there are eight equally spaced contours, plus an additional contour corresponding to $u = 0$ in parts (b) and (c). In each part regions of downwards flow (i.e. $u > 0$) are shaded in grey while regions of upwards flow (i.e. $u < 0$) are unshaded. The locations of the maximum and/or minimum velocity are marked with dots ($\bullet$) and/or open circles ($\circ$), respectively. Note that the length of the axes and the contour interval are different in each part of this figure.

but upwards elsewhere, where the semi-width of the region of downwards flow, b ($< a$), is given by (11), and the semi-width of the region in which there is downwards flow all the way across the rivulet, c ($< b$), is given by (12). In particular, this means that in this case the free-surface velocity satisfies $u_{\rm s} > 0$ for $|y| < c$, $u_{\rm s} = 0$ at $|y| = c$, and $u_{\rm s} < 0$ for $c < |y| < a$. We refer to this more interesting flow pattern as type II behaviour (Figure 4b).

When $a = -4\tau$ we have $H_{\rm m} = h_{\rm m} = -2\tau$, $b = -2\sqrt{2}\tau$ and $c = 0$, and the region of downwards flow just touches the free surface at $y = 0$. We refer to this flow pattern as type III behaviour (Figure 4c). Type III behaviour is intermediate between the type II behaviour described above and the type IV behaviour described below.

When $-2\tau < a < -4\tau$ we have $0 < H_{\rm m} < h_{\rm m}$ and the velocity is downwards in the region

$$0 < z < H \quad \text{for} \quad |y| < b, \tag{14}$$

but upwards elsewhere. We refer to this flow pattern as type IV behaviour (Figure 4d). Note that both the solution $a = a_0 = -7\tau/2$ for which $Q = 0$ and the solution $a = a_{\rm min} = -21\tau/8$ for which $Q = Q_{\rm min}$ lie in this interval and hence both have type IV behaviour.

When $a > -2\tau$ the maximum velocity $u_{\rm max} = (a + 2\tau)^2/8$ (> 0) occurs within the flow at $y = 0$ and $z = h_{\rm m} + \tau = (a + 2\tau)/2$, and the minimum velocity $u_{\rm min} = -\tau^2/2$ (< 0) occurs on the free surface at $y = \pm b$ and $z = -\tau$. In particular, this means that when the flow pattern is of type II the location of $u_{\rm max}$ lies further from the substrate than the location of

$u_{\min}$, but that the situation is reversed when it is of type IV. In the special case of type III behaviour the locations of $u_{\min}$ and $u_{\max}$ lie at exactly the same distance from the substrate.

Finally, when $a \leq -2\tau$ we have $H_{\rm m} \leq 0$ and the velocity is always upwards throughout the rivulet, and the minimum velocity $u_{\min} = u_{\rm s}(0) = a(a+4\tau)/8$ (< 0) occurs on the free surface at $y = 0$ and $z = h_{\rm m} = a/2$. We refer to this final possible flow pattern as type V behaviour (Figure 4e).

As previously mentioned, Figure 4 shows sketches of the flow patterns of types I–V. In particular, Figure 4 shows the regions of upwards flow and downwards flow, and the locations of $u_{\max}$ and/or $u_{\min}$. Figure 5 shows plots of the contours of u for several values of Q and τ illustrating examples of flow patterns of types I, II, IV and V. Note that the flow patterns shown in parts (c) and (d) of Figure 5 have the same flux Q and prescribed shear stress τ, but different semi-widths a.

The different flow patterns that can occur when $\tau < 0$ can be understood by recalling from (7) that the local downwards flux due to gravity varies with h like h^3 while the local upwards flux due to shear stress varies like h^2. Thus in the thinnest part of the rivulet (and, in particular, near the edges where $h = 0$) the effect of shear is always stronger than that due to gravity and the flow is always upwards. However, if the rivulet is sufficiently thick (specifically, if $h > -\tau$) then the effect of gravity is stronger than that due to shear stress near the substrate (which is furthest away from the free surface where the shear stress is acting) and so the flow there is downwards. If the rivulet is even thicker (specifically, if $h > -2\tau$) then the effect of gravity is sufficiently strong to make the fluid flow downwards all the way across the rivulet.

4 Prescribed Semi-Width $a = \bar{a}$

If a takes the prescribed positive value $\bar{a} > 0$ then, as Figures 1 and 2 show, there is a unique solution for Q for all values of τ. In particular, in the special case of no prescribed shear stress ($\tau = 0$) the flux of a purely gravity-driven rivulet is given by $Q = 4\bar{a}^4/105$.

Figure 6 shows a sketch of Q as a function of a and summarises when the different types of flow pattern occur for $\tau > 0$, $\tau = 0$ and $\tau < 0$. Specifically, Figure 6 shows that when $\tau \geq 0$ the solution is always of type I, but that when $\tau < 0$ the solution is of type II for $a > -4\tau$, type III when $a = -4\tau$, type IV for $-2\tau < a < -4\tau$, and type V for $0 < a \leq -2\tau$. Figure 6 also shows that the flux is negative when $\tau < 0$ and $a < a_0$, zero when $\tau < 0$ and $a = a_0$, but positive otherwise.

Since in this case the shape of the rivulet is independent of τ, increasing (decreasing) the value of τ from zero has the effect of increasing (decreasing) the velocity u and hence increasing (decreasing) the flux Q.

5 Prescribed Flux $Q = \bar{Q}$

If Q takes the prescribed value $\bar{Q}$ (which may be positive, negative or zero) then, as Figures 1 and 3 show, the number of solutions for a depends on the sign of τ and the value of $\bar{Q}$. When $\tau \geq 0$ there is one solution for all positive values of $\bar{Q}$, but no solution when $\bar{Q}$ is zero or negative. On the other hand, when $\tau < 0$ there is one solution for $\bar{Q} \geq 0$, two solutions for $Q_{\min} < \bar{Q} < 0$ (the narrower one satisfying $0 \leq a < a_{\min}$ and the wider one $a_{\min} < a \leq a_0$), one solution $a = a_{\min}$ when $\bar{Q} = Q_{\min}$, and no solution when $\bar{Q} < Q_{\min}$, where $Q_{\min}$ is given by (9). In particular, in the special case of no prescribed shear stress ($\tau = 0$) we recover the explicit expression for the semi-width of a purely gravity-driven rivulet obtained by Duffy and Moffatt [16], namely $a = (105\bar{Q}/4)^{1/4}$.

Figure 7 shows a sketch of a as a function of τ and summarises when the different types of

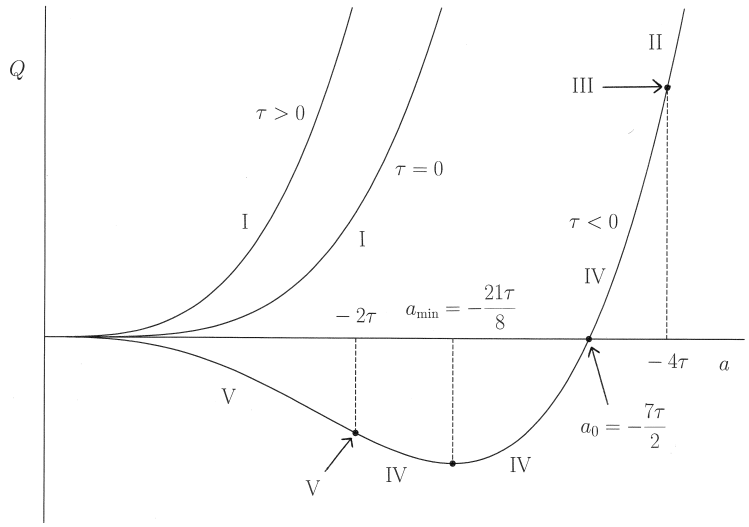

Figure 6: Sketch of Q as a function of a summarising when the different types of flow pattern occur for $\tau > 0$, $\tau = 0$ and $\tau < 0$.

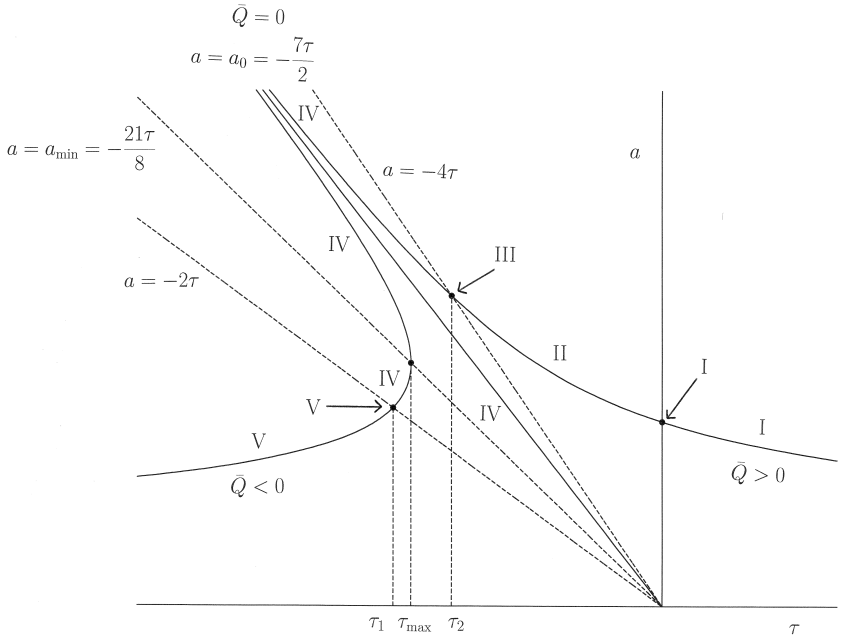

Figure 7: Sketch of a as a function of τ summarising when the different types of flow pattern occur for $\bar{Q} > 0$, $\bar{Q} = 0$ and $\bar{Q} < 0$.

flow pattern occur for $\bar{Q} > 0$, $\bar{Q} = 0$ and $\bar{Q} < 0$. Specifically, Figure 7 shows that when $\bar{Q} > 0$ there is one solution for all values of τ and the semi-width of this solution is a monotonically decreasing function of τ. This solution is of type I for $\tau \geq 0$, type II for $\tau_2 < \tau < 0$, type III when $\tau = \tau_2$, and type IV for $\tau < \tau_2$, where τ_2 (< 0) is given by

$$\tau_2 = -\left(\frac{105\bar{Q}}{128}\right)^{\frac{1}{4}}. \tag{15}$$

Figure 7 also shows that when $\bar{Q} < 0$ there are two solutions for $\tau < \tau_{\max}$ (the narrower of which is a monotonically increasing function of τ, and the wider of which is a monotonically decreasing function of τ), one when $\tau = \tau_{\max}$, and none for $\tau > \tau_{\max}$, where $\tau_{\max}$ (< 0) is given by

$$\tau_{\max} = -\left(-\frac{5120\bar{Q}}{3087}\right)^{\frac{1}{4}}. \tag{16}$$

For $\tau \leq \tau_1$ the narrower solution is of type V, where τ_1 ($< \tau_{\max}$) is given by

$$\tau_1 = -\left(-\frac{35\bar{Q}}{16}\right)^{\frac{1}{4}}, \tag{17}$$

but all the other solutions are of type IV. Figure 7 also shows that the solution in the special case $\bar{Q} = 0$ is always of type IV.

In the limit of small positive flux $\bar{Q} \to 0^+$ for $\tau > 0$ or small negative flux $\bar{Q} \to 0^-$ for $\tau < 0$ there is always a solution that becomes narrow (and shallow) according to

$$a \sim \left(\frac{15\bar{Q}}{2\tau}\right)^{\frac{1}{3}} \to 0^+. \tag{18}$$

When $\tau < 0$ there are two solutions in the limit of small negative flux $\bar{Q} \to 0^-$, and the semi-width of the wider solution approaches the finite value $a = a_0 = -7\tau/2$ according to

$$a = -\frac{7\tau}{2} - \frac{30\bar{Q}}{49\tau^3} + O(\bar{Q}^2\tau^{-7}). \tag{19}$$

In the limit of large positive flux, $\bar{Q} \to \infty$, the rivulet always becomes wide (and deep) according to

$$a = \left(\frac{105\bar{Q}}{4}\right)^{\frac{1}{4}} - \frac{7\tau}{8} + O(\bar{Q}^{-\frac{1}{4}}\tau^2). \tag{20}$$

for all values of τ. There is, of course, no solution in the limit of large negative flux, $\bar{Q} \to -\infty$.

In the limit of small shear stress, $\tau \to 0$, the solution is a regular perturbation about the solution in the case $\tau = 0$ and is given by (20). In the limit of large positive shear stress, $\tau \to \infty$, the effect of the shear stress overwhelms that of gravity and the rivulet becomes narrow (and shallow) according to (18) when $\bar{Q} > 0$. However, the behaviour in the limit of large negative shear stress, $\tau \to -\infty$, is somewhat more complicated. Whereas for the narrower solution when $\bar{Q} < 0$ the effect of the shear stress overwhelms that of gravity and the rivulet again becomes narrow (and shallow) according to (18), for both the wider solution when $\bar{Q} < 0$ and the solution when $\bar{Q} > 0$ the effects of shear stress and gravity balance each other at leading order and the rivulet becomes wide (and deep) according to (19).

Unlike in the case of prescribed semi-width $a = \bar{a}$ described in the previous section, in the case of prescribed flux $Q = \bar{Q}$ the shape of the rivulet depends on τ via a, and so the dependence of a on τ is somewhat more complicated than the dependence of Q on τ described

previously. When $\tau > 0$ the velocity is always downwards and the effect of increasing the shear stress from zero is always to increase the local velocity of the fluid throughout the rivulet (i.e. $\partial u/\partial\tau > 0$ everywhere). Hence, since the flux must remain constant, the rivulet always becomes narrower (and shallower), i.e. $\partial a/\partial\tau = -7a/(8a + 21\tau) < 0$. As we have already seen, when $\tau < 0$ the situation is somewhat more complicated. In particular, the velocity is always upwards near the edges of the rivulet, but may be downwards elsewhere. Moreover, the effect of decreasing the shear stress from zero can be either to increase or to decrease the local velocity. (Specifically, $\partial u/\partial\tau > 0$ everywhere both when $0 < a < a_{\min}$ and when $a > -21\tau$, $\partial u/\partial\tau < 0$ everywhere when $a_{\min} < a < -14\tau/3$, but $\partial u/\partial\tau$ is positive is some parts of the rivulet and negative in others when $-14\tau/3 < a < -21\tau$.) However, the net effect of the changes to the size of the rivulet and to the velocity along it are that when $a < a_{\min}$ the rivulet always becomes narrower (and shallower), i.e. $\partial a/\partial\tau > 0$, whereas when $a > a_{\min}$ it always becomes wider (and deeper), i.e. $\partial a/\partial\tau < 0$.

6 Stability

A full stability analysis of the rivulets described here is beyond the scope of the present work, but in the case of prescribed flux $Q = \bar{Q}$ we can make useful progress by generalising the quasi-steady stability analysis of a purely gravity-driven rivulet undertaken by Wilson and Duffy [17]. Following the earlier work we assume that the flow remains symmetric and unidirectional and that the quasi-steady motion is driven entirely by that of the moving contact line $y = A$, where $A = A(t)$. Furthermore, we assume that the speed of the moving contact line, A', and the dynamic contact angle, $\theta = \theta(t)$, are related by a general "Tanner law" in the form $A' = F(\theta)$, where the function $F(\theta)$ satisfies $F(1) = 0$ and is monotonically increasing near $\theta = 1$. Perturbing about the constant steady-state values of the semi-width and the contact angle $A = a$ and $\theta = 1$ by writing $A = a + a_1(t)$ and $\theta = 1 + \theta_1(t)$, and making use of the fact that the perturbed rivulet must also satisfy the prescribed volume-flux condition $Q = \bar{Q}$, yields

$$a_1' = \frac{M(\lambda a_1)^m}{m!}, \tag{21}$$

where $M = \mathrm{d}^m F/\mathrm{d}\theta^m|_{\theta=1} > 0$ ($m = 1, 3, 5, \ldots$) is the first non-zero derivative of $F(\theta)$ evaluated at $\theta = 1$ and

$$\lambda = -\left.\frac{Q_A}{Q_\theta}\right|_{A=a,\,\theta=1} = -\frac{8a + 21\tau}{2a(3a + 7\tau)}. \tag{22}$$

Equation (21) can be immediately solved for a_1 and this solution shows that, whatever the specific form of $F(\theta)$, the stability of the rivulet depends only on the sign of λ. Specifically, the rivulet is unstable to small perturbations when $\lambda > 0$ and stable when $\lambda < 0$. Thus we can immediately deduce that when $\tau \geq 0$ the rivulet is always stable, but when $\tau < 0$ the rivulet is unstable when $-7\tau/3 < a < a_{\min} = -21\tau/8$. Specifically when $\tau < 0$ and $\bar{Q} \geq 0$ the rivulet is always stable, but when $\tau < 0$ and $Q_{\min} \leq \bar{Q} < 0$ the wider rivulet is always stable while the narrower rivulet is stable when $0 < a < -7\tau/3$ but unstable when $-7\tau/3 < a < a_{\min}$.

7 Rivulet Splitting

Myers *et al.* [14] addressed the question of whether or not it is ever energetically favourable for a rivulet to split into two or more subrivulets. In this section we revisit this problem and in so doing correct and extend the results they obtained. In particular, we shall calculate when it is energetically favourable for a rivulet driven by gravity and/or a prescribed shear stress to split.

The total energy of the rivulet is the sum of its kinetic energy and surface energy. Momentarily reverting to dimensional variables, the kinetic energy (per unit length) is given by

$$\frac{\rho}{2}\int_{-a}^{+a}\int_{0}^{h} u^2 \,\mathrm{d}z\,\mathrm{d}y \tag{23}$$

and the surface energy, or, more precisely, the difference between the surface energy of the rivulet and the surface energy of the dry substrate (per unit length) is given by

$$\gamma\left[\int_{-a}^{+a}(1+h'^2)^{\frac{1}{2}}\,\mathrm{d}y - 2a\cos\beta\right] \tag{24}$$

(see, for example, Mikielewicz and Moszynski [11], Myers *et al.* [14], and Saber and El-Genk [10]). Thus, if we non-dimensionalise energy (per unit length) with $\rho U^2\beta l^2 = \rho^3 g^2\beta^5 l^6/\mu^2$ then the leading-order expression for the energy of the thin rivulet on a vertical substrate considered in the present work, E, is given by

$$E = \int_{-a}^{+a}\frac{h^5}{15} + \frac{5\tau h^4}{24} + \frac{\tau^2 h^3}{6}\,\mathrm{d}y + \frac{1}{W}\left[\frac{1}{2}\int_{-a}^{+a} h'^2\,\mathrm{d}y + a\right], \tag{25}$$

which can be evaluated explicitly to yield

$$E = \frac{16a^6}{10395} + \frac{2\tau a^5}{189} + \frac{2\tau^2 a^4}{105} + \frac{4a}{3W}, \tag{26}$$

where

$$W = \frac{\rho l U^2}{\gamma\beta} = \frac{\gamma^2\beta^3}{gl\mu^2} \tag{27}$$

is an appropriately defined Weber number (a non-dimensional measure of the relative importance of surface energy and kinetic energy). The expression for the kinetic energy in (26) is in agreement with the appropriate limit of the corresponding result given by Myers *et al.* [14, Equation 40] if the typographical error in their coefficient a_2 is corrected (specifically, their mL should be $\sqrt{C}$). The expression for the surface energy in (26) corrects the corresponding result given by Myers *et al.* [14, Equation 41], who mistakenly omitted a contribution due to the surface energy of the free surface. In addition, it should be noted that, since the flow is rectilinear, the inertia terms in the governing equations are *identically zero* and so the comments made by Myers *et al.* [14] about the restriction on the applicability of the thin-film approximation are erroneous: the present analysis (and, in particular, the present expression for E) is valid for *all* values of the Reynolds number.

It can readily be demonstrated that (for a fixed value of τ) E is a monotonically increasing function of a. Thus wider rivulets always have more energy than narrower ones, and hence it is *never* energetically favourable for a rivulet to split into one or more *wider* rivulets. However, it can be energetically favourable for a rivulet to split into one or more *narrower* rivulets. Specifically, it is energetically favourable for a rivulet with semi-width a and flux Q to split into two rivulets, one with semi-width a_q and flux q ($0 < q \leq Q/2$) and the other with semi-width a_{Q-q} and flux $Q-q$, if the difference between the energies of the two states, ΔE, defined by

$$\Delta E = E - \left[E(a=a_q) + E(a=a_{Q-q})\right], \tag{28}$$

is positive.

7.1 Purely Gravity-Driven Case

In the special case of a purely gravity-driven rivulet (i.e. the case $\tau = 0$) the semi-width is given explicitly in terms of the flux by $a = (105Q/4)^{1/4}$, and when $a < a_{\mathrm{c}}$ (or equivalently

when $Q < Q_{\rm c}$) then $\Delta E < 0$ for all $0 < q \le Q/2$, but when $a = a_{\rm c}$ ($Q = Q_{\rm c}$) then $\Delta E = 0$ at $q = Q/2$, and when $a > a_{\rm c}$ ($Q > Q_{\rm c}$) then $\Delta E > 0$ in an interval $Q/2 - q^* < q \le Q/2$, where q^* (> 0) is a monotonically increasing function of Q. Thus for $a > a_{\rm c}$ (or equivalently for $Q > Q_{\rm c}$) it is energetically favourable for the rivulet to split into two narrower rivulets, where the critical values of the semi-width, $a_{\rm c}$, and the flux, $Q_{\rm c}$, are given by

$$a_{\rm c} = \left[\frac{3465(2^{\frac{3}{4}} - 1)}{4(1 - 2^{-\frac{1}{2}})W}\right]^{\frac{1}{5}} \simeq \frac{4.5805}{W^{\frac{1}{5}}}, \quad Q_{\rm c} = \frac{4}{105}\left[\frac{3465(2^{\frac{3}{4}} - 1)}{4(1 - 2^{-\frac{1}{2}})W}\right]^{\frac{4}{5}} \simeq \frac{16.7703}{W^{\frac{4}{5}}}. \tag{29}$$

This result agrees qualitatively with the work of Myers *et al.* [14], who calculated $a_{\rm c}$ and $Q_{\rm c}$ numerically for a range of values of β.

7.2 Purely Shear-Stress-Driven Case

In the limit of large positive shear stress $\tau \to \infty$ when $Q > 0$, and for the narrower rivulet in the limit of large negative shear stress $\tau \to -\infty$ when $Q < 0$, the leading order semi-width is given by $a = (15Q/2\tau)^{1/3}$, and the behaviour of ΔE is qualitatively the same as that in the case $\tau = 0$ described above, and the critical values of the semi-width and the flux are now given by

$$a_{\rm c} = \left[\frac{70(2^{\frac{2}{3}} - 1)}{(1 - 2^{-\frac{1}{3}})\tau^2 W}\right]^{\frac{1}{3}} \simeq \frac{5.8413}{\tau^{\frac{2}{3}} W^{\frac{1}{3}}}, \quad Q_{\rm c} = \frac{28(2^{\frac{2}{3}} - 1)}{3(1 - 2^{-\frac{1}{3}})\tau W} \simeq \frac{26.5750}{\tau W}. \tag{30}$$

In particular, this result shows that the conjecture proposed by Myers *et al.* [14] on the basis of their numerical calculations that it is *never* energetically favourable for a purely shear-stress-driven rivulet to split is *not* correct.

7.3 General Case

When both gravity and shear-stress effects are significant analytical progress is harder. However, we can still make progress numerically. Before doing this it is convenient to remove W from the problem by scaling a with $W^{-1/5}$, τ with $W^{-1/5}$, Q with $W^{-4/5}$, and E with $W^{-6/5}$. When $Q > 0$ the behaviour is qualitatively the same as that in the case $\tau = 0$, i.e. there are critical values of the semi-width, $a_{\rm c}$, and the flux, $Q_{\rm c}$, above which it is energetically favourable for a rivulet to split into two narrower rivulets, and the critical situation is that of splitting into two equal rivulets each with half the flux of the original, i.e. the case $q = Q/2$. When $Q_{\rm min} \le Q < 0$ (which is possible only when $\tau < 0$) the situation is somewhat more complicated. In this case there are always two possible rivulets with the same flux (the narrower one satisfying $0 < a \le a_{\rm min}$ and the wider one $a_{\rm min} < a < a_0$). As we have already seen, it is *always* energetically favourable for the wider rivulet to "split" into the narrower rivulet with the same flux. On the other hand, the behaviour of the narrower rivulet is somewhat similar to that of the rivulets in the case $Q > 0$ described previously. Specifically, for $\tau_{\rm c} \le \tau < 0$, where $\tau_{\rm c}$ is found numerically to be approximately equal to $-2.5038\,W^{-1/5}$, it is never energetically favourable for the smaller rivulet to split, but for $\tau < \tau_{\rm c}$ there is a critical value of the semi-width $a_{\rm c}$ ($0 < a_{\rm c} \le a_{\rm min}$) above which and a critical value of the flux $Q_{\rm c}$ ($Q_{\rm min} \le Q_{\rm c} < 0$) below which it is energetically favourable for the rivulet to split into two narrower rivulets, and the critical situation is again that of splitting into two equal rivulets each with half the flux of the original, i.e. the case $q = Q/2$. In all cases the values of $a_{\rm c}$ and $Q_{\rm c}$ can be determined numerically by calculating the values of a and Q for which $\Delta E = 0$ at $q = Q/2$. Note that $a_{\rm c} = a_{\rm min}(\tau_{\rm c}) \simeq 6.5725\,W^{-1/5}$ and $Q_{\rm c} = Q_{\rm min}(\tau_{\rm c}) \simeq -23.6954\,W^{-4/5}$.

Figures 8 and 9 show $W^{1/5}a$ and $W^{4/5}Q$, respectively, plotted as functions of $W^{1/5}\tau$ and indicate when it is energetically favourable and when it is energetically unfavourable for a

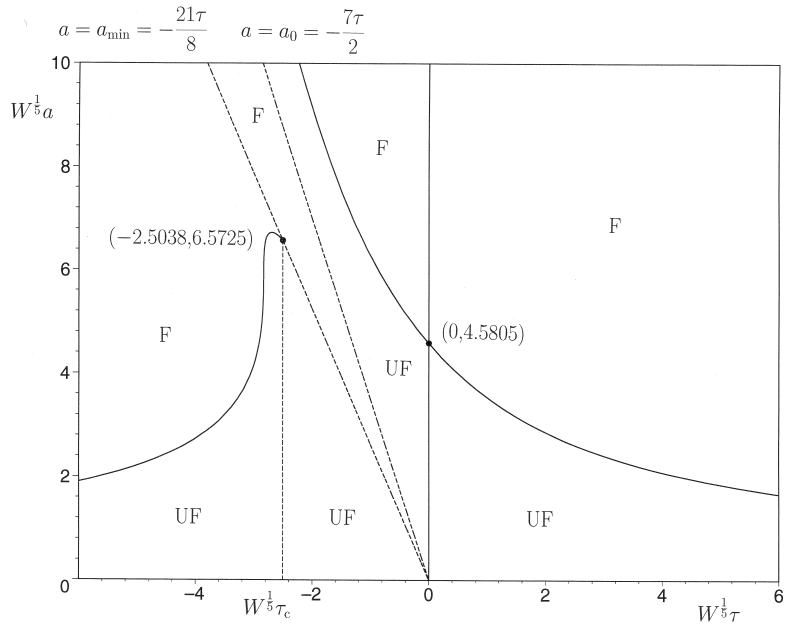

Figure 8: Plot of $W^{1/5}a$ as a function of $W^{1/5}\tau$ indicating when it is energetically favourable (denoted by "F") and when it is energetically unfavourable (denoted by "UF") for a rivulet to split. The curves $a = a_{\min} = -21\tau/8$ and $a = a_0 = -7\tau/2$ are indicated with dashed lines.

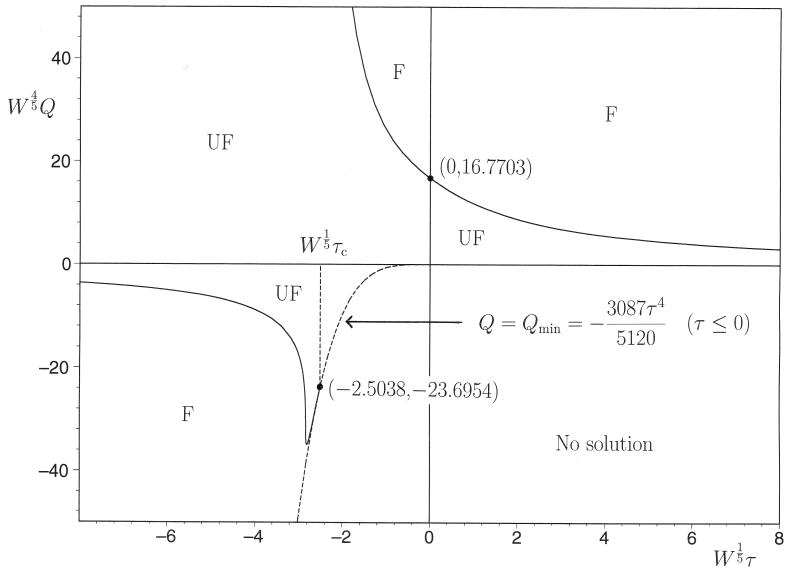

Figure 9: Plot of $W^{4/5}Q$ as a function of $W^{1/5}\tau$ indicating when it is energetically favourable (denoted by "F") and when it is energetically unfavourable (denoted by "UF") for a rivulet to split. The curve $Q = Q_{\min} = -3087\tau^4/5120$ in $\tau \le 0$ is indicated with a dashed line. Note that when $\tau < 0$ and $Q_{\min} < Q < 0$ the region in which it is unfavourable to split applies only to the narrower rivulet.

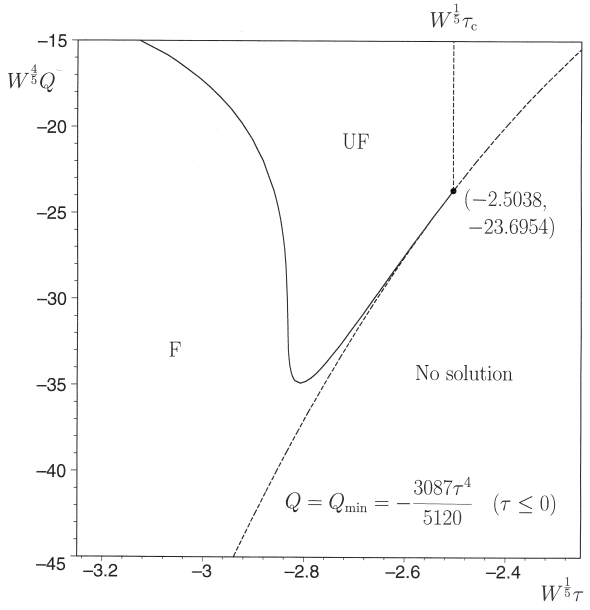

Figure 10: Enlargement of Figure 9 showing the detail near $\tau = \tau_c$.

rivulet to split. Figure 10 shows the detail of Figure 9 near $\tau = \tau_c$ where there is a narrow region in which it is favourable for a rivulet to split that is difficult to discern on the original figure. When interpreting Figures 9 and 10 it should be remembered that when $\tau < 0$ and $Q_{\min} < Q < 0$ there are two possible rivulets with the same flux and, since it is always favourable for the wider rivulet to split, the region in which it is unfavourable to split shown in Figures 9 and 10 applies only to the narrower rivulet.

8 Conclusions

In the present paper we used the lubrication approximation to obtain a complete description of the steady unidirectional flow of a thin rivulet on a vertical substrate subject to a prescribed uniform longitudinal shear stress at its free surface. We interpreted the solution we obtained both as a rivulet with prescribed semi-width $a = \bar{a}$ but unknown flux Q, and as a rivulet with prescribed flux $Q = \bar{Q}$ but unknown semi-width a; the results are summarised in Figures 6 and 7, respectively. In particular, in the case of prescribed flux we found that when $\tau \ge 0$ there is one possible rivulet solution for $\bar{Q} > 0$, but no solution when $\bar{Q} \le 0$. On the other hand, when $\tau < 0$ there is one possible rivulet solution for $\bar{Q} \ge 0$, two solutions for $Q_{\min} < \bar{Q} < 0$ (the narrower one with $0 \le a < a_{\min}$ and the wider one $a_{\min} < a \le a_0$), one solution with $a = a_{\min}$ when $\bar{Q} = Q_{\min}$, and no solution when $\bar{Q} < Q_{\min}$. We systematically categorised and analysed all of the possible flow patterns and found that whereas for $\tau \ge 0$ the velocity is always downwards throughout the rivulet, when $\tau < 0$ the velocity is always upwards near the edges of the rivulet, but it can be downwards elsewhere. In particular, when $a \le -2\tau$ the velocity is always upwards throughout the rivulet. We determined the quasi-steady stability of a rivulet in the case of prescribed flux and found that the rivulet is always stable except when $\tau < 0$ and $Q_{\min} \le \bar{Q} < 0$, in which case the narrower rivulet is stable when $0 < a < -7\tau/3$ but unstable when $-7\tau/3 < a < a_{\min}$. We also calculated when it is energetically favourable for a rivulet to split into two narrower rivulets, and the results are summarised in Figures 8 and 9.

Thus far all the results have been presented in terms of non-dimensional quantities for clarity and simplicity. It is, however, informative to translate these results into dimensional terms. For example, for rivulets of water (with, say, $\rho = 10^3$ kg m^{-3}, $\mu = 10^{-3}$ N s m^{-2}, $\gamma = 70 \times 10^{-3}$ N m^{-1}, and $\beta = 30°$) and of a silicone oil (with, say, $\rho = 10^3$ kg m^{-3}, $\mu = 20 \times 10^{-3}$ N s m^{-2}, $\gamma = 20 \times 10^{-3}$ N m^{-1}, and $\beta = 40°$) the widths of both a purely gravity-driven rivulet with volume flux 1 cm^3 s^{-1} (typical of the volume fluxes investigated by Hewitt and Lacey [18] and Schmuki and Laso [15]) and a rivulet with zero net volume flux with prescribed (upwards) shear stress 10 N m^{-2} (typical of the shear stresses investigated by Hewitt and Lacey [18]) are all around 0.5 cm. Furthermore, the magnitude of the minimum value of the flux when the prescribed (upwards) shear stress is 10 N m^{-2} is around 10 cm^3 s^{-1} for water, but is an order of magnitude smaller for the silicone oil.

Note that, although perhaps slightly obscured by the choice of non-dimensionalisation, the results described in the present work include the very simple special case of a purely shear-stress-driven rivulet. Specifically, if we revert to dimensional variables and set $g = 0$ then we have $u = \tau z/\mu$, $u_{\rm S} = \tau h/\mu$, $\bar{u} = \tau h^2/2\mu$ and $Q = 2\tau\beta^2 a^3/15\mu$. In this case there is always single rivulet for each value of $\bar{a}$ (> 0) or $\bar{Q}$ (provided that it has the same sign as τ), and the flow is always in the same direction as the prescribed shear stress throughout the rivulet (i.e. the flow pattern is always of type I when $\tau > 0$ and always of type V when $\tau < 0$). As expected, all of these results coincide with the leading-order behaviour of the solutions described in the present paper in the limit of large positive shear stress when $Q > 0$ and large negative shear stress when $Q < 0$.

The present analysis is restricted to the simplest case of steady unidirectional flow, but in practice a variety of more complicated phenomena, including break-up into drops, and both steady and unsteady rivulet meandering, can also occur. Nevertheless, as the series of experiments on rivulet flow in the absence of a prescribed shear stress undertaken by Schmuki and Laso [15] show, there is a significant region of parameter space in which steady unidirectional flow occurs.

Acknowledgement

Both authors acknowledge interesting discussions with Ms Laura Fariss (formerly of the Department of Mathematics, University of Strathclyde) concerning rivulets with significant surface-shear forces.

References

[1] J. A. Moriarty, L. W. Schwartz, and E. O. Tuck, "Unsteady spreading of thin liquid films with small surface tension," *Phys. Fluids A* **3**, 733–742 (1991).
[2] A. C. King and E. O. Tuck, "Thin liquid layers supported by steady air-flow surface traction," *J. Fluid Mech.* **251**, 709–718 (1993).
[3] A. C. King, E. O. Tuck, and J.-M. Vanden-Broeck, "Air-blown waves on thin viscous sheets," *Phys. Fluids A* **5**, 973–978 (1993).
[4] J. J. Kriegsmann, M. J. Miksis, and J.-M. Vanden-Broeck, "Pressure driven disturbances on a thin viscous film," *Phys. Fluids* **10**, 1249–1255 (1998).
[5] I. S. McKinley, S. K. Wilson, and B. R. Duffy, "Spin coating and air-jet blowing of thin viscous drops," *Phys. Fluids* **11**, 30–47 (1999).
[6] T. G. Myers, J. P. F. Charpin, and C. P. Thompson, "Slowly accreting ice due to supercooled water impacting on a cold surface," *Phys. Fluids* **14**, 240–256 (2002).
[7] M. Villegas-Díaz, H. Power, and D. S. Riley, "On the stability of rimming flows to two-dimensional disturbances," *Fluid Dyn. Res.* **33**, 141–172 (2003).

[8] G. J. B. Black, "Theoretical Studies of Thin-Film Flows," M. Phil. Thesis, University of Strathclyde, Glasgow, UK, 2002.
[9] S. K. Wilson, B. R. Duffy, and G. J. B. Black, "Thin-film flow on a stationary or uniformly rotating horizontal cylinder subject to a prescribed uniform shear stress at the free surface of the film" Submitted for publication (2004).
[10] H. H. Saber and M. S. El-Genk, "On the breakup of a thin liquid film subject to interfacial shear," *J. Fluid Mech.* **500**, 113–133 (2004).
[11] J. Mikielewicz and J. R. Moszynski, "An improved analysis of breakdown of thin liquid films," *Archives of Mechanics* **30**, 489–500 (1978).
[12] M. H. Eres, L. W. Schwartz, and R. V. Roy, "Fingering phenomena for driven coating films," *Phys. Fluids* **12**, 1278–1295 (2000).
[13] S. K. Wilson, B. R. Duffy, and R. Hunt, "A slender rivulet of a power-law fluid driven by either gravity or a constant shear stress at the free surface," *Q. J. Mech. Appl. Math.* **55**, 385–408 (2002).
[14] T. G. Myers, H. X. Liang, and B. Wetton, "The stability and flow of a rivulet driven by interfacial shear and gravity," *Int. J. Non-Linear Mech.* **39**, 1239–1249 (2004).
[15] P. Schmuki and M. Laso, "On the stability of rivulet flow," *J. Fluid Mech.* **215**, 125–143 (1990).
[16] B. R. Duffy and H. K. Moffatt, "Flow of a viscous trickle on a slowly varying incline," *Chem. Eng. J.* **60**, 141–146 (1995).
[17] S. K. Wilson and B. R. Duffy, "On the gravity-driven draining of a rivulet of viscous fluid down a slowly varying substrate with variation transverse to the direction of flow," *Phys. Fluids* **10**, 13–22 (1998).
[18] G. F. Hewitt and P. M. C. Lacey, "The breakdown of the liquid film in annular two-phase flow," *Int. J. Heat Mass Transfer* **8**, 781–791 (1965).